Published in final edited form as:
Epilepsy Res. 2012 June ; 100(0): 93–103. doi:10.1016/j.eplepsyres.2012.01.012.

The antiepileptic drug mephobarbital is not transported by P-glycoprotein or multidrug resistance protein 1 at the blood-brain barrier: a positron emission tomography study

Severin Mairinger[a,b,c,&], **Jens P. Bankstahl**[d,e,&], **Claudia Kuntner**[a], **Kerstin Römermann**[d], **Marion Bankstahl**[d], **Thomas Wanek**[a], **Johann Stanek**[a,c], **Wolfgang Löscher**[d], **Markus Müller**[c], **Thomas Erker**[b,*], and **Oliver Langer**[a,c,§]

[a]Health & Environment Department, Molecular Medicine, AIT Austrian Institute of Technology GmbH, Seibersdorf, Austria

[b]Department of Medicinal Chemistry, University of Vienna, Austria

[c]Department of Clinical Pharmacology, Medical University of Vienna, Austria

[d]Department of Pharmacology, Toxicology & Pharmacy, University of Veterinary Medicine Hannover, Germany

[e]Clinic of Nuclear Medicine, Hannover Medical School, Hannover, Germany

Summary

Aim of this study was to determine whether the carbon-11-labelled antiepileptic drug [^{11}C]mephobarbital is a substrate of P-glycoprotein (Pgp) and can be used to assess Pgp function at the blood-brain barrier (BBB) with positron emission tomography (PET). We performed paired PET scans in rats, wild-type (FVB) and *Mdr1a/b*$^{(-/-)}$ mice, before and after intravenous administration of the Pgp inhibitor tariquidar (15 mg/kg). Brain-to-blood AUC_{0-60} ratios in rats and brain AUC_{0-60} values of [^{11}C]mephobarbital in wild-type and *Mdr1a/b*$^{(-/-)}$ mice were similar in scan 1 and scan 2, respectively, suggesting that *in vivo* brain distribution of [^{11}C]mephobarbital is not influenced by Pgp efflux. Absence of Pgp transport was confirmed *in vitro* by performing concentration equilibrium transport assay in cell lines transfected with *MDR1* or *Mdr1a*. PET experiments in wild-type mice, with and without pretreatment with the multidrug resistance protein (MRP) inhibitor MK571 (20 mg/kg), and in *Mrp1*$^{(-/-)}$ mice suggested that [^{11}C]mephobarbital is also not transported by MRPs at the murine BBB, which was also supported by *in vitro* transport experiments using human *MRP1*-transfected cells. Our results are surprising as phenobarbital, the *N*-desmethyl derivative of mephobarbital, has been shown to be a substrate of Pgp, which suggests that *N*-methylation abolishes Pgp affinity of barbiturates.

Keywords

drug resistance; epilepsy; blood-brain barrier; P-glycoprotein; PET; [^{11}C]mephobarbital

[*]*Corresponding author:* Tel.: +43-1-4277-550 03; fax: +43-1-4277-9 551. thomas.erker@univie.ac.at.
[&]These two authors contributed equally to this study.
[§]oliver.langer@ait.ac.at (O. Langer)

Conflicts of interest None of the authors has any conflict of interest to disclose. The authors confirm that they have read the Journal's position on issues involved in ethical publication and affirm that this manuscript is consistent with those guidelines.

Appendix A. Supplementary data Supplementary data associated with this article can be found in the online version.

Europe PMC Funders Author Manuscripts

Introduction

Approximately 30% of epilepsy patients do not respond to treatment with antiepileptic drugs (AED), which may have severe consequences, such as shortened lifespan, bodily injury, neuropsychological and psychiatric impairment, and social disability (Regesta and Tanganelli 1999). According to the transporter hypothesis of drug resistance lack of treatment response is caused by a regional overexpression of the adenosine triphosphate binding cassette (ABC) transporters P-glycoprotein (Pgp, MDR1, ABCB1) and multidrug resistance proteins (MRPs) in epileptic brain tissue, which impede access of AEDs to their pharmacological target sites inside the brain by active efflux transport across the blood-brain barrier (BBB) (Löscher and Potschka 2005a; Remy and Beck 2006). Although most AEDs seem to be better transported by murine than by human Pgp (Baltes et al. 2007b), it has now become widely accepted that several clinically used AEDs, notably phenytoin and phenobarbital (Fig. 1), are weak substrates of human Pgp (Luna-Tortós et al. 2008; Zhang et al. 2010; Zhang et al. 2011). Recent studies in rat models of therapy resistant epilepsy have shown that animals, which initially did not respond to treatment with phenytoin or phenobarbital, became treatment responsive when the potent third-generation Pgp inhibitor tariquidar (XR9576) (Fox and Bates 2007) was co-administered (Brandt et al. 2006; van Vliet et al. 2006). These experiments support the notion that treatment of therapy refractory epilepsy patients with Pgp modulators such as tariquidar might be a promising strategy to overcome drug resistance in the clinic.

A non-invasive molecular imaging protocol which allows for assessing function and/or expression of cerebral Pgp *in vivo* would be clinically useful for identifying epilepsy patients whose resistance is caused by altered Pgp function/expression, prior to initiation of Pgp modulating treatment (Mairinger et al. 2011). The nuclear imaging method positron emission tomography (PET) has shown great promise to assess Pgp function at the BBB of animals and humans *in vivo* (Kannan et al. 2009; Mairinger et al. 2011). However, so far PET imaging protocols have relied on the use of high affinity Pgp substrates, such as racemic [^{11}C]verapamil, (*R*)-[^{11}C]verapamil or [^{11}C]-*N*-desmethyl-loperamide (Kannan et al. 2009; Mairinger et al. 2011). These radiotracers are efficiently transported by Pgp at the BBB resulting in very low brain uptake, which makes them unsuitable to detect regionally increased Pgp function in the epileptic brain as this will lead to further reductions in PET signal. We have recently shown in a rat model of regional cerebral Pgp overexpression (Bankstahl and Löscher 2008) that performing (*R*)-[^{11}C]verapamil PET scans after half-maximum inhibition of Pgp by tariquidar results in higher brain PET signals and is better suited than (*R*)-[^{11}C]verapamil baseline scans to measure Pgp function in the brain (Bankstahl et al. 2011). However, this approach requires pretreatment of study subjects with therapeutic doses of tariquidar (Wagner et al. 2009), which might be difficult to accomplish in a routine clinical PET imaging setting and which is also hampered by the restricted availability of tariquidar for clinical use.

A promising alternative strategy to visualize cerebral Pgp function would be the use of low affinity Pgp substrates, which should in principle display better brain entry than high affinity substrates, under conditions when Pgp is fully functional (i.e. without administration of a Pgp inhibitor prior to the PET scan). An attractive choice as candidate compounds for PET tracer development are in fact AEDs, as most of them are highly permeable, low molecular weight, lipophilic molecules with much weaker Pgp transport affinities as compared to classical Pgp substrates such as digoxin or vinblastine (Luna-Tortós et al. 2008). The use of radiolabelled AEDs for PET imaging additionally offers the benefit that direct assessment of brain concentration levels of AEDs in humans is expected to be clinically more relevant to predict treatment response than the use of surrogate markers of Pgp function, such as (*R*)-[^{11}C]verapamil or [^{11}C]-*N*-desmethyl-loperamide.

Almost 30 years ago, first attempts have been made to radiolabel phenytoin with ^{11}C and assess its brain distribution in epilepsy patients (Roeda and Westera 1981; Baron et al. 1983). However, a detailed regional assessment of [^{11}C]phenytoin kinetics in brain was hampered by the low spatial resolution of PET cameras available at that time. Moreover, the applicability of [^{11}C]phenytoin PET is restricted as its radiochemical synthesis requires the use of [^{11}C]phosgene as a synthetic intermediate (Roeda and Westera 1981), which is not routinely available in most clinical PET centers. The *N*-methyl analogue of phenobarbital, methylphenobarbital (mephobarbital, Fig. 1), has until recently been used in the US under the brand name Mebaral^{TM} as a sedative, anxiolytic and anticonvulsant with similar indications as phenobarbital. Mephobarbital potentially gives straightforward access to ^{11}C-labelling by *N*-methylation of phenobarbital using standard radiochemical procedures available in most PET radiochemistry laboratories. Due to its close structural similarity with phenobarbital (Fig. 1), one would expect that mephobarbital will also be transported by Pgp. Aim of this study was to synthesize for the first time [^{11}C]mephobarbital and to assess its suitability to visualize Pgp function at the BBB by performing small-animal PET experiments in rats and mice. To confirm the *in vivo* data, *in vitro* transcellular transport assays using human and murine Pgp or human MRP1 overexpressing cells were performed.

Methods

Chemicals

All chemicals were purchased from Sigma-Aldrich Chemie (Schnelldorf, Germany) and Merck KGaA (Darmstadt, Germany) at analytical grade and used without further purification. Tariquidar dimesylate was obtained from Xenova Ltd. (Slough, UK). For administration, tariquidar was freshly dissolved on each experimental day in 2.5% (w/v) aqueous (aq) dextrose solution and injected intravenously (iv) at volumes of 2 and 4 mL/kg into rats and mice, respectively. MK571 sodium salt hydrate (Sigma-Aldrich Chemie) was dissolved in 1.25% (w/v) aq sodium hydrogencarbonate solution and iv injected at a volume of 4 mL/kg into mice. [^{14}C]Mannitol was purchased from Hartmann Analytic (Braunschweig, Germany). [^{11}C]Methane was produced *via* the $^{14}N(p,\alpha)^{11}C$ nuclear reaction by irradiating nitrogen gas containing 10% hydrogen using a PETtrace cyclotron equipped with a methane target system (GE Healthcare, Uppsala, Sweden). [^{11}C]Methyl iodide was prepared *via* the gas-phase method (Larsen et al. 1997) in a TracerLab FXC Pro synthesis module (GE Healthcare) and converted into [^{11}C]methyl triflate by passage through a column containing silver-triflate impregnated graphitized carbon (Jewett 1992).

Animals

Adult female Sprague Dawley rats weighing 267±3 g were obtained from Harlan Netherlands (Horst, Netherlands). Female FVB (wild-type), *Mdr1a/b*$^{(-/-)}$ and *Mrp1*$^{(-/-)}$ mice weighing 27±3 g were purchased from Taconic Inc. (Germantown, NY, USA). The study was approved by the local Animal Welfare Committee and all study procedures were performed in accordance with the Austrian Animal Experiments Act. Animals had access to food and water *ad libitum* and were kept under a 12 h light/dark cycle.

Cell lines and cell cultures

LLC-PK1 cells transfected with human *MDR1* (LLC-*MDR1*) or *MRP1* (LLC-*MRP1*), murine *Mdr1a* (LLC-*Mdr1a*) and respective wild-type LLC cells were kindly provided by Prof. P. Borst (The Netherlands Cancer Institute, Amsterdam, Netherlands). Cells were cultured as described in detail previously (Baltes et al. 2007a; Baltes et al. 2007b). Shortly, after thawing from liquid nitrogen, cells were used within a maximum of 13 passages after receiving them. The cell lines were regularly tested for vincristine resistance (640 nmoL) before being used for transport experiments (compare (Baltes et al. 2007a)).

Synthesis of [^{11}C]mephobarbital

Using a TracerLab FXC Pro synthesis module [^{11}C]methyl triflate was bubbled through a solution of phenobarbital (0.5 mg, 2.2 μmol) in acetone (0.5 mL). After heating for 3 min at 60°C the reaction mixture was cooled (25°C), diluted with water (0.5 mL) and injected into a built-in high-performance liquid chromatography (HPLC) system equipped with a Chromolith Performance RP-18e (100-4.6 mm) column (Merck KGaA) which was eluted with methanol/water (17/83, v/v) at a flow rate of 5 mL/min. The HPLC eluate was monitored in series for radioactivity and ultraviolet (UV) absorption at a wavelength of 227 nm. On this system, radiolabelling precursor phenobarbital and product [^{11}C]mephobarbital eluted with retention times of 2-5 min and 7-10 min, respectively. The product fraction collected from HPLC was diluted with water (100 mL) and passed over a C18 Sep-Pak Plus cartridge (Waters, Milford, MA, USA), which had been pre-activated with ethanol (5 mL) and water (10 mL). The cartridge was then washed with water (10 mL) followed by elution of [^{11}C]mephobarbital with ethanol (3 mL). The ethanol was then removed by heating at 80°C under a stream of argon and the product was formulated in a mixture of 0.9% aq saline/0.1 M sodium hydroxide (1/0.011, v/v) at an approximate concentration of 370 MBq/mL for iv injection into animals. [^{11}C]Mephobarbital ready for iv injection was obtained in a decay-corrected radiochemical yield based on [^{11}C]methane of 6±4% (n = 21) in a total synthesis time of 37 min.

Radiochemical purity and specific activity of [^{11}C]mephobarbital were determined by analytical radio-HPLC using a LiChrospher 100 RP-18e (250-4 mm, 5 μm) column eluted with methanol/water (50/50, v/v) at a flow rate of 1 mL/min. UV detection was performed at a wavelength of 210 nm. The retention time of [^{11}C]mephobarbital was approximately 10 min on this HPLC system. The identity of [^{11}C]mephobarbital was confirmed by HPLC co-injection with unlabelled mephobarbital. Radiochemical purity of [^{11}C]mephobarbital was >98% and specific activity at end of synthesis was >50 GBq/μmol.

Small-animal PET imaging and PET data analysis

Animals were kept under anesthesia with 1.5-2% isoflurane administered *via* a mask during the whole experiment. They were continuously warmed at around 37°C. Rats were implanted with catheters into the femoral artery (for blood sampling) and vein (for administration of [^{11}C]mephobarbital and tariquidar). In mice, a lateral tail vein was used for radiotracer and unlabelled inhibitor administration. The animals were positioned in the imaging chamber and [^{11}C]mephobarbital (rats: 58±12 MBq in a volume of about 0.25 mL, containing < 1.5 nmol of unlabelled mephobarbital; mice: 30±7 MBq in a volume of about 0.1 mL, containing < 1 nmol of unlabelled mephobarbital) was administered as an iv bolus over approximately 30 s. At the start of radiotracer injection, dynamic PET imaging was initiated using a microPET Focus220 scanner (Siemens, Medical Solutions, Knoxville, USA).

The employed study set-up is illustrated in Figure 2. Rats (n = 3) underwent paired PET scans with [^{11}C]mephobarbital, before and after administration of tariquidar (15 mg/kg). Tariquidar was injected iv over approximately 60 s at 60 min after start of scan 1, which was followed by further 90 min of PET data acquisition. Scan 2 was performed at 2 h after injection of tariquidar. During both PET scans, 5 μL arterial blood samples were withdrawn manually with pre-weighted micropipettes from the femoral artery (approximately every 5 s) during the first 3 min after radiotracer injection, followed by further 10 μL samples taken at 5, 10, 20, 30, 40, 50, 60, 70, 80 and 90 min (last three time points for scan 1 only).

In analogy to rats, wild-type mice and *Mdr1a/b*$^{(-/-)}$ mice (n = 3 each) underwent paired PET scans with [^{11}C]mephobarbital, before and after administration of tariquidar (15 mg/kg).

Two additional groups of wild-type mice underwent single 60-min PET scans with [^{11}C]mephobarbital without (n = 4) and with (n = 3) pretreatment with MK571 (20 mg/kg) which was injected iv over 30 s at 30 min before start of the PET scan. One group of *Mrp1*$^{(-/-)}$ mice (n = 4) underwent single 60-min PET scans with [^{11}C]mephobarbital. In the three groups of mice which underwent only single 60-min PET scans blood was collected at the end of the scan by retro-orbital puncture using pre-weighted micropipettes. As blood sampling was not feasible during the paired scan set-up separate groups of wild-type mice and *Mdr1a/b*$^{(-/-)}$ mice (n = 3 each) were injected under isoflurane-anesthesia with [^{11}C]mephobarbital (11±5 MBq) before and after administration of tariquidar (15 mg/kg) and venous blood was sampled at 25 and 60 min after each radiotracer injection by retro-orbital puncture using pre-weighted micropipettes.

Blood samples of rats and mice were weighted and counted for activity in a 1-detector Wallac gamma counter (Perkin Elmer Instruments, Wellesley, USA), which had been cross-calibrated with the PET camera. Blood activity data were corrected for radioactive decay and normalized to injected dose per gram body weight and expressed as standardized uptake value (SUV = (radioactivity per mL/injected radioactivity) x body weight).

PET images were reconstructed by Fourier rebinning followed by 2-dimensional filtered back projection with a ramp filter. The standard data correction protocol (normalization, attenuation, decay correction and injection decay correction) was applied to the data. Whole brain was manually outlined on multiple planes of the PET summation images using the image analysis software Amide and time-activity curves (TACs), expressed as SUV, were calculated. From brain TACs (rats and mice) and blood TACs (rats only) the areas under the TACs from 0 to 60 min after radiotracer injection (AUC_{0-60}) were calculated. For rats, brain-to-blood AUC_{0-60} ratios were obtained by dividing AUC_{0-60} in brain through AUC_{0-60} in blood.

Analysis of metabolites and plasma protein binding of [^{11}C]mephobarbital

A separate group of rats (n = 5), which did not undergo PET scanning, was injected under isoflurane-anesthesia with [^{11}C]mephobarbital (117±69 MBq in a volume of about 0.3 mL) for metabolite analysis. At 40 min after radiotracer injection, rats were sacrificed, a terminal blood sample (5 mL) collected and their brains removed. Blood was centrifuged to obtain plasma (3000xg, 5 min, 21°C), counted for radioactivity in the 1-detector Wallac gamma counter and analyzed for radiolabelled metabolites of [^{11}C]mephobarbital using a modified version of a previously described solid-phase extraction (SPE)/HPLC assay (Abrahim et al. 2008). In brief, arterial plasma was diluted with water (1 mL), spiked with a solution of unlabelled mephobarbital in dimethylsulfoxide (10 mg/mL, 20 μL) and acidified with 5M aq hydrochloric acid (80 μL) and loaded on a Sep-Pak vac tC18 cartridge (Waters Corporation, Milford, USA), which had been pre-activated with methanol (3 mL) and water (5 mL). The cartridge was first washed with water (4 mL) and then eluted with methanol (4 mL). Radioactivity in all three fractions (plasma, water, methanol) was measured in the gamma counter. More than 99% of total radioactivity in rat plasma was recovered in the methanol fraction. The methanol fraction was 2:1 (v/v) diluted with water and further analyzed by HPLC using a Chromolith Performance RP 18-e (100-4.6 mm) column, which was eluted at 25°C with methanol/water (17/83, v/v) at a flow rate of 4 mL/min (injected volume: 2 mL). UV detection was performed at 214 nm. An unidentified polar radiolabelled metabolite of [^{11}C]mephobarbital and unchanged [^{11}C]mephobarbital eluted with retention times of 1-2 and 14-16 min, respectively. For validation of the SPE assay, [^{11}C]mephobarbital dissolved in water (0.5 mL) was subjected to the SPE procedure showing that all radioactivity was quantitatively recovered in the methanol fraction. Plasma protein binding of [^{11}C]mephobarbital was determined by ultrafiltration of fresh rat plasma samples, which had been incubated with [^{11}C]mephobarbital, using Amicon Microcon YM-10 centrifugal filter

devices (Millipore Corporation, Bedford, MA, USA), essentially as described previously for (*R*)-[^{11}C]verapamil (Kuntner et al. 2010).

Rat brain was washed twice with ice-cold water and homogenized in 0.9% aq sodium chloride solution (0.8 mL) using an IKA T10 basic Ultra-turrax (IKA Laboratory Equipment, Staufen, Germany). The brain homogenate was spiked with unlabelled mephobarbital, mixed with acetonitrile (1.5 mL) and centrifuged (3 min, 4 °C, 13,000g). The supernatant was diluted 1:1 (v/v) with water and injected into the same HPLC system as used for analysis of radiolabelled metabolites in plasma (injected volume: 2 mL).

Transcellular transport assays

Cell culture experiments were described in detail recently (Baltes et al. 2007a; Baltes et al. 2007b; Luna-Tortós et al. 2008). Cells were seeded at a density of 0.3×10^6 cells/cm^2 on transparent polyester membrane filters (Transwell-Clear®, 6-well, 24 mm diameter, 0.4 mm pore size, Corning Costar Corporation, Cambridge, MA, USA), cultured for 1-2 days to confluence and transport assays were performed between days 5 and 7 after confluence. The culture medium was replaced with Opti-MEM® (Gibco™/Invitrogen Corporation, Eggenstein, Germany) before starting the transport experiments, and the transwells were pre-incubated for 1 h (with or without Pgp or MRP inhibitors tariquidar, 0.5 μM or MK571, 50 μM, respectively). In the beginning of each transport study mephobarbital was applied at a concentration of 50 μM to apical and basolateral sides of the monolayer with fresh Opti-MEM®, so that initial drug concentration was the same in both compartments. This procedure has been termed “concentration equilibrium transport assay” and has recently been shown to identify Pgp transport of highly permeable drugs such as phenobarbital (Luna-Tortós et al. 2008; Zhang et al. 2010). In experiments with Pgp inhibitor, tariquidar was also added to both chambers. Each experiment was performed in triplicate, where the volumes in the upper and lower compartment were 2000 μL and 2700 μL, respectively. For drug analysis, samples were taken at 60, 120, 240, and 360 min from both compartments. Pre-incubation and following transport assays were performed at 37°C in a humidified incubator (5% CO_2) with shaking the transwells gently at 50 rpm. Integrity of monolayers was determined by measuring transepithelial electrical resistance (TEER) and [^{14}C]mannitol permeability (Luna-Tortós et al. 2008). As positive control transport of racemic verapamil (0.5 μM) was assessed in LLC-*MDR1* and LLC-*Mdr1a* cells and transport of calcein-AM (1 μM) in LLC-*MRP1* cells as described previously (Luna-Tortós et al. 2010; Löscher et al. 2011).

Concentrations of mephobarbital were measured by HPLC with UV-detection at 210 nm by a modification of the method previously used for phenobarbital (Potschka et al. 2002). Limit of quantification for mephobarbital was 31.3 ng/mL. Analysis of transport data was performed as described earlier (Luna-Tortós et al. 2008).

Statistical analysis

For all outcome parameters from *in vivo* experiments, differences between groups were tested with two-tailed paired or unpaired Student’s t-tests using PRISM 5 software (GraphPad Software Inc., La Jolla, CA, USA). Statistical significance of differences in cell culture experiments was calculated by two-way analysis of variance (ANOVA) for repeated measures, followed by Bonferroni post-tests. If not stated otherwise, results are shown as mean ± standard deviation (SD). The level of statistical significance was set to $p < 0.05$.

Results

Small-animal PET experiments

To determine whether active Pgp-mediated efflux affects [^{11}C]mephobarbital distribution across the BBB *in vivo* we performed paired PET scans in rats, wild-type mice and *Mdr1a/b*$^{(-/-)}$ mice, before and after administration of the Pgp inhibitor tariquidar (15 mg/kg). Peak brain activity uptake (SUV) in rats was 3.1±0.2 in scan 1 and 3.1±1.0 in scan 2, at about 1 min following injection of [^{11}C]mephobarbital (Fig. 3a, b). Brain and blood TACs in scan 1 did not change in response to tariquidar administration and were at similar levels as in scan 2. Activity distribution in rat brain after injection of [^{11}C]mephobarbital appeared uniform without obvious regional differentiation (Fig. 3c). Pgp inhibition did neither alter [^{11}C]mephobarbital brain concentrations nor brain-to-blood $AUC_{0\text{-}60}$ ratios (scan 1: 2.0±0.5; scan 2: 2.4±0.3) (Fig. 3d). Radio-HPLC analysis of brain tissue extracts collected at 40 min after injection of [^{11}C]mephobarbital in a separate group of rats (n = 5) showed that 96±6% of total activity in brain was in the form of unchanged [^{11}C]mephobarbital. In rat plasma, >85% of total activity was unchanged [^{11}C]mephobarbital with an unidentified polar radiolabelled metabolite eluting with the void volume of the HPLC column. The fraction of unbound [^{11}C]mephobarbital in rat plasma was 0.21±0.05 (n = 3).

Similar results were obtained in paired PET scans in wild-type and *Mdr1a/b*$^{(-/-)}$ mice (Fig. 4). Again, brain TACs of both groups of mice were similar in scan 1 and scan 2 and showed no changes in response to tariquidar administration during scan 1 (Fig. 4a, b). Brain $AUC_{0\text{-}60}$ values were not significantly different between wild-type and *Mdr1a/b*$^{(-/-)}$ mice, in scan 1 and scan 2, respectively, but significantly decreased in scan 2 relative to scan 1 in wild-type animals (p = 0.013) (Fig. 4c). Blood activity concentrations were similar except for wild-type scan 1 25 min *versus* wild-type scan 2 25 min (p = 0.048), wild-type scan 1 60 min *versus Mdr1a/b*$^{(-/-)}$ scan 1 60 min (p = 0.042) and wild-type scan 2 60 min *versus Mdr1a/b*$^{(-/-)}$ scan 2 60 min (p = 0.040).

To assess whether active efflux transport by MRPs influences brain distribution of [^{11}C]mephobarbital, we performed PET scans in wild-type mice without and with administration of the MRP inhibitor MK571 (20 mg/kg) (Fig. 5). In addition, PET scans were performed in *Mrp1*$^{(-/-)}$ mice. Brain uptake did neither differ between untreated and MK571 pretreated mice (Fig. 5a, c) nor wild-type and *Mrp1*$^{(-/-)}$ mice (Fig. 5b, c). Moreover, blood activity concentrations at 60 min after radiotracer injection were similar in all three groups of animals (Fig. 5d).

In vitro transport experiments

Transport of mephobarbital was assessed *in vitro* across monolayers of wild-type LLC cells and LLC cells transfected with human *MDR1*, *MRP1* or murine *Mdr1a* employing concentration equilibrium conditions in which mephobarbital was initially added in identical concentrations (50 μM) to both the apical and the basolateral chamber (Fig. 6). For all cell types, mephobarbital concentrations in both compartments remained stable and close to initial concentrations over the time course of the experiment (6 h) indicating lack of active transport of mephobarbital by Pgp or MRP1 from the basolateral to the apical compartment. Addition of tariquidar (0.5 μM) or MK571 (50 μM), respectively, did not change concentrations in both compartments over time as compared with control experiments. In analogy to the PET control data (see supplementary data), the functional activity of Mdr1a and MDR1 was demonstrated by using the Pgp substrate verapamil, which clearly showed basolateral-to-apical transport which could be inhibited by addition of tariquidar (for Mdr1a, exemplarily shown in Fig. 6f). The functional activity of MRP1 was demonstrated by using the MRP1 substrate calcein-AM (data not shown).

Discussion

In the present study we evaluated for the first time the brain distribution of a radiolabelled AED *in vivo* in rodents with PET imaging, before and after administration of the potent Pgp inhibitor tariquidar at a dose (15 mg/kg) which has been shown before to completely inhibit Pgp at the BBB in naïve rats (Kuntner et al. 2010). As a parameter for BBB penetration of [^{11}C]mephobarbital we calculated the brain-to-blood $AUC_{0\text{-}60}$ ratio in rats (Fig. 3d), which is comparable to $K_{p,\ brain}$, the brain-to-plasma concentration ratio, commonly used in drug development to assess BBB penetration (Hammarlund-Udenaes et al. 2008), provided that the contribution of radiolabelled metabolites to the PET signal is small. We have shown that total radioactivity concentrations measured in brain and plasma mainly represented unchanged parent compound suggesting that [^{11}C]mephobarbital is hardly metabolized in rats during the time course of the 1 h PET scan.

In the present study we used the same set-up (see Fig. 2) as in the *in vivo* evaluation of the high affinity Pgp substrate (*R*)-[^{11}C]verapamil in rats (Kuntner et al. 2010). (*R*)-[^{11}C]verapamil was shown to have relatively low brain uptake in baseline scans without tariquidar administration, with brain-to-blood $AUC_{0\text{-}60}$ ratios close to 1 (Kuntner et al. 2010) (see Supplementary Fig. S1). In immediate response to tariquidar injection during scan 1 a steep rise in brain TACs of (*R*)-[^{11}C]verapamil was observed, reaching concentration values which were up to 5 times higher than values before tariquidar administration, with no apparent changes in blood activity levels (Kuntner et al. 2010). In scan 2, brain-to-blood $AUC_{0\text{-}60}$ ratio of (*R*)-[^{11}C]verapamil was 8 times increased relative to scan 1 (see Supplementary Fig. S1). In line with our assumption that mephobarbital is a permeable molecule, a two times higher brain-to-blood $AUC_{0\text{-}60}$ ratio was obtained for [^{11}C]mephobarbital in scan 1 as compared to (*R*)-[^{11}C]verapamil (Supplementary Fig. S1). However, contrary to our observations with (*R*)-[^{11}C]verapamil, for [^{11}C]mephobarbital we did not find significant differences between brain-to-blood $AUC_{0\text{-}60}$ ratios in scan 1 and 2 (Supplementary Fig. S1), suggesting that Pgp efflux transport does not influence brain distribution of [^{11}C]mephobarbital in rats.

In mice we obtained similar results, both with chemical knockout of Pgp by tariquidar and with genetic knockout of Pgp by using *Mdr1a/b*$^{(-/-)}$ mice. Due to the small blood volume of mice, arterial blood sampling during the PET scan is not possible, which prohibited the determination of brain-to-blood $AUC_{0\text{-}60}$ ratios as we had done in rats. Instead, blood concentrations were assessed at two time points in a separate group of mice which did not undergo PET scanning (Fig. 4d). Again very similar brain TACs and brain $AUC_{0\text{-}60}$ values for wild-type and *Mdr1a/b*$^{(-/-)}$ mice, both in scan 1 and scan 2, suggested absence of Pgp efflux of [^{11}C]mephobarbital at the BBB (Fig 4). The exact reasons for the higher blood activity levels in *Mdr1a/b*$^{(-/-)}$ mice than in wild-type mice at 60 min after tracer injection are not known (Fig. 4d). However, these differences in blood activity levels do not affect the interpretation of the study results as they would result in decreased brain-to-blood ratios of [^{11}C]mephobarbital in *Mdr1a/b*$^{(-/-)}$ mice as compared to wild-type mice. (*R*)-[^{11}C]verapamil, on the other hand, had shown in the same set-up 5.3 times higher brain $AUC_{0\text{-}60}$ values in *Mdr1a/b*$^{(-/-)}$ than in wild-type mice in scan 1 and no differences in $AUC_{0\text{-}60}$ values between *Mdr1a/b*$^{(-/-)}$ and wild-type mice in scan 2 (see Supplementary Fig. S2).

To corroborate our unexpected *in vivo* findings we assessed Pgp transport of unlabelled mephobarbital *in vitro* using monolayers of LLC cells overexpressing either human or murine Pgp (Fig. 6). As it has previously been demonstrated that the conventional bidirectional transport assay often fails to identify highly permeable compounds like AEDs as Pgp substrates due to their passive back-diffusion into the donor compartment, we

employed the concentration equilibrium transport assay, in which the influence of passive diffusion is minimized by adding the drug at equal concentrations to the apical and the basolateral compartments (Luna-Tortós et al. 2008). Using this assay, it has recently been shown that phenobarbital is transported by MDR1, which can be partly inhibited (54%) by addition of tariquidar (0.5 μM) (Luna-Tortós et al. 2008). Contrary to the results obtained with phenobarbital, we failed to identify significant transport of mephobarbital by Pgp using identical assay conditions as for phenobarbital (Fig. 6). These *in vitro* and *in vivo* findings are surprising as Pgp is known to transport a wide range of structurally diverse molecules and mephobarbital structurally differs from phenobarbital only with respect to an *N*-methyl group in the barbituric acid moiety (Fig. 1). It therefore appears likely that both N-H groups are essential for binding of phenobarbital to Pgp, possibly by hydrogen bonding. However, as it has been reported that metabolism of mephobarbital occurs in part by *N*-demethylation yielding phenobarbital as active metabolite (Butler et al. 1952), Pgp efflux may still be involved in resistance to mephobarbital.

A previous study had shown that transport of phenobarbital across monolayers of *MDR1*-transfected LLC cells could be blocked to a higher extent by the MRP inhibitor MK571 than by tariquidar, suggesting that phenobarbital might be, in addition to Pgp, actively transported by endogenously expressed MRPs in LLC cells (Luna-Tortós et al. 2008). Subsequent experiments in MDCKII cells selectively transfected with *MRP1*, *MRP2* or *MRP5*, however, failed to demonstrate significant transport of phenobarbital by any of these MRP subtypes (Luna-Tortós et al. 2010). To investigate whether MRP-mediated transport of [^{11}C]mephobarbital occurs at the BBB *in vivo*, we performed PET scans in wild-type mice, with and without pretreatment with MK571, as well as in *Mrp1*$^{(-/-)}$ mice (Fig. 5). MK571, which was originally developed as a leukotriene receptor antagonist for treatment of asthma (Margolskee 1991), is known to inhibit MRPs, without being MRP subtype-specific (Löscher and Potschka 2005b; Luna-Tortós et al. 2010). Although MK571 has been used before to inhibit MRPs *in vitro* (Dallas et al. 2003; Luna-Tortós et al. 2010), we are not aware of any *in vivo* studies using MK571 as an MRP inhibitor. The MK571 dose employed in our experiments (20 mg/kg) was several times higher than doses used for treatment of asthma and should have resulted in plasma levels of MK571 which were above its *in vitro* half-inhibitory concentration (IC_{50}) of MRP2 (10 μM) (Margolskee 1991; Matsson et al. 2009). Our experiments showed no effect of MK571 pretreatment or Mrp1 knockout on brain uptake of [^{11}C]mephobarbital (Fig. 5) arguing against the possibility that MRP-mediated transport of mephobarbital at the BBB plays a significant role *in vivo*. Again, *in vitro* transport assays supported this conclusion (Fig. 6 d,e).

In conclusion, we found no evidence for Pgp transport of mephobarbital, both at the rodent BBB *in vivo* and in transcellular transport experiments *in vitro*, suggesting that [^{11}C]mephobarbital is not suitable as a PET tracer for Pgp function. Future efforts will be therefore directed at the synthesis of [^{11}C]phenobarbital, which will be characterized using the same *in vivo* set-up as [^{11}C]mephobarbital.

Supplementary Material

Refer to Web version on PubMed Central for supplementary material.

Acknowledgments

The research leading to these results has received funding from the European Community's Seventh Framework Programme (FP7/2007-2013) under grant agreement number 201380 ("Euripides"), the Austrian Science Fund (FWF) project "Transmembrane Transporters in Health and Disease" (SFB F35) and the "Hochschuljubiläumsstiftung der Stadt Wien" (project H-2139/2010). The authors would like to thank Michael Sauberer (AIT), Florian Bauer and Bernd Dörner (both University of Vienna) for technical support.

References

Abrahim A, Luurtsema G, Bauer M, Karch R, Lubberink M, Pataraia E, Joukhadar C, Kletter K, Lammertsma AA, Baumgartner C, Müller M, Langer O. Peripheral metabolism of (R)-[^{11}C]verapamil in epilepsy patients. Eur. J. Nucl. Med. Mol. Imaging. 2008; 35:116–123. [PubMed: 17846766]

Baltes S, Fedrowitz M, Tortós CL, Potschka H, Löscher W. Valproic acid is not a substrate for P-glycoprotein or multidrug resistance proteins 1 and 2 in a number of in vitro and in vivo transport assays. J. Pharmacol. Exp. Ther. 2007a; 320(1):331–343. [PubMed: 17043155]

Baltes S, Gastens AM, Fedrowitz M, Potschka H, Kaever V, Löscher W. Differences in the transport of the antiepileptic drugs phenytoin, levetiracetam and carbamazepine by human and mouse P-glycoprotein. Neuropharmacology. 2007b; 52(2):333–346. [PubMed: 17045309]

Bankstahl JP, Löscher W. Resistance to antiepileptic drugs and expression of P-glycoprotein in two rat models of status epilepticus. Epilepsy Res. 2008; 82(1):70–85. [PubMed: 18760905]

Bankstahl JP, Bankstahl M, Kuntner C, Stanek J, Wanek T, Meier M, Ding X, Müller M, Langer O, Löscher W. A novel PET imaging protocol identifies seizure-induced regional overactivity of P-glycoprotein at the blood-brain barrier. J. Neurosci. 2011; 31(24):8803–8811. [PubMed: 21677164]

Baron JC, Roeda D, Munari C, Crouzel C, Chodkiewicz JP, Comar D. Brain regional pharmacokinetics of ^{11}C-labeled diphenylhydantoin: positron emission tomography in humans. Neurology. 1983; 33(5):580–585. [PubMed: 6601779]

Brandt C, Bethmann K, Gastens AM, Löscher W. The multidrug transporter hypothesis of drug resistance in epilepsy: Proof-of-principle in a rat model of temporal lobe epilepsy. Neurobiol. Dis. 2006; 24(1):202–211. [PubMed: 16928449]

Butler TC, Mahaffee D, Mahaffee C. The role of the liver in the metabolic disposition of mephoparbital. J. Pharmacol. Exp. Ther. 1952; 106(3):364–369. [PubMed: 13000633]

Dallas S, Zhu X, Baruchel S, Schlichter L, Bendayan R. Functional expression of the multidrug resistance protein 1 in microglia. J. Pharmacol. Exp. Ther. 2003; 307(1):282–290. [PubMed: 12893836]

Fox E, Bates SE. Tariquidar (XR9576): a P-glycoprotein drug efflux pump inhibitor. Expert Rev. Anticancer Ther. 2007; 7(4):447–459. [PubMed: 17428165]

Hammarlund-Udenaes M, Friden M, Syvänen S, Gupta A. On the rate and extent of drug delivery to the brain. Pharm. Res. 2008; 25(8):1737–1750. [PubMed: 18058202]

Jewett DM. A simple synthesis of [^{11}C]methyl triflate. Appl. Radiat. Isot. 1992; 43:1383–1385.

Kannan P, John C, Zoghbi SS, Halldin C, Gottesman MM, Innis RB, Hall MD. Imaging the function of P-glycoprotein with radiotracers: pharmacokinetics and in vivo applications. Clin. Pharmacol. Ther. 2009; 86(4):368–377. [PubMed: 19625998]

Kuntner C, Bankstahl JP, Bankstahl M, Stanek J, Wanek T, Stundner G, Karch R, Brauner R, Meier M, Ding XQ, Müller M, Löscher W, Langer O. Dose-response assessment of tariquidar and elacridar and regional quantification of P-glycoprotein inhibition at the rat blood-brain barrier using (R)-[^{11}C]verapamil PET. Eur. J. Nucl. Med. Mol. Imaging. 2010; 37(5):942–953. [PubMed: 20016890]

Larsen P, Ulin J, Dahlstrøm K, Jensen M. Synthesis of [^{11}C]iodomethane by iodination of [^{11}C]methane. Appl. Radiat. Isot. 1997; 48(2):153–157.

Löscher W, Potschka H. Drug resistance in brain diseases and the role of drug efflux transporters. Nat. Rev. Neurosci. 2005a; 6(8):591–602. [PubMed: 16025095]

Löscher W, Potschka H. Role of drug efflux transporters in the brain for drug disposition and treatment of brain diseases. Prog. Neurobiol. 2005b; 76(1):22–76. [PubMed: 16011870]

Löscher W, Luna-Tortós C, Romermann K, Fedrowitz M. Do ATP-binding cassette transporters cause pharmacoresistance in epilepsy? Problems and approaches in determining which antiepileptic drugs are affected. Curr. Pharm. Des. 2011; 17(26):2808–2828. [PubMed: 21827408]

Luna-Tortós C, Fedrowitz M, Löscher W. Several major antiepileptic drugs are substrates for human P-glycoprotein. Neuropharmacology. 2008; 55(8):1364–1375. [PubMed: 18824002]

Luna-Tortós C, Fedrowitz M, Löscher W. Evaluation of transport of common antiepileptic drugs by human multidrug resistance-associated proteins (MRP1, 2 and 5) that are overexpressed in pharmacoresistant epilepsy. Neuropharmacology. 2010; 58(7):1019–1032. [PubMed: 20080116]

Mairinger S, Erker T, Müller M, Langer O. PET and SPECT radiotracers to assess function and expression of ABC transporters in vivo. Curr. Drug Metabol. 2011; 12(5):774–792.

Margolskee DJ. Clinical experience with MK-571. A potent and specific LTD4 receptor antagonist. Ann. N. Y. Acad. Sci. 1991; 629:148–156. [PubMed: 1659276]

Matsson P, Pedersen JM, Norinder U, Bergström CA, Artursson P. Identification of novel specific and general inhibitors of the three major human ATP-binding cassette transporters P-gp, BCRP and MRP2 among registered drugs. Pharm. Res. 2009; 26(8):1816–1831. [PubMed: 19421845]

Potschka H, Fedrowitz M, Löscher W. P-Glycoprotein-mediated efflux of phenobarbital, lamotrigine, and felbamate at the blood-brain barrier: evidence from microdialysis experiments in rats. Neurosci. Lett. 2002; 327(3):173–176. [PubMed: 12113905]

Regesta G, Tanganelli P. Clinical aspects and biological bases of drug-resistant epilepsies. Epilepsy Res. 1999; 34(2-3):109–122. [PubMed: 10210025]

Remy S, Beck H. Molecular and cellular mechanisms of pharmacoresistance in epilepsy. Brain. 2006; 129(Pt 1):18–35. [PubMed: 16317026]

Roeda D, Westera G. The Synthesis of Some C-11-Labeled Anti-Epileptic Drugs with Potential Utility as Radiopharmaceuticals - Hydantoins and Barbiturates. Int. J. Appl. Radiat. Isot. 1981; 32(11): 843–845. [PubMed: 7309275]

van Vliet EA, van Schaik R, Edelbroek PM, Redeker S, Aronica E, Wadman WJ, Marchi N, Vezzani A, Gorter JA. Inhibition of the multidrug transporter P-glycoprotein improves seizure control in phenytoin-treated chronic epileptic rats. Epilepsia. 2006; 47(4):672–680. [PubMed: 16650133]

Wagner CC, Bauer M, Karch R, Feurstein T, Kopp S, Chiba P, Kletter K, Löscher W, Müller M, Zeitlinger M, Langer O. A pilot study to assess the efficacy of tariquidar to inhibit P-glycoprotein at the human blood-brain barrier with (R)–^{11}C-verapamil and PET. J. Nucl. Med. 2009; 50(12): 1954–1961. [PubMed: 19910428]

Zhang C, Kwan P, Zuo Z, Baum L. In vitro concentration dependent transport of phenytoin and phenobarbital, but not ethosuximide, by human P-glycoprotein. Life Sci. 2010; 86(23-24):899–905. [PubMed: 20417647]

Zhang C, Zuo Z, Kwan P, Baum L. In vitro transport profile of carbamazepine, oxcarbazepine, eslicarbazepine acetate, and their active metabolites by human P-glycoprotein. Epilepsia. 2011; 52(10):1894–1904. [PubMed: 21692796]

Europe PMC Funders Author Manuscripts

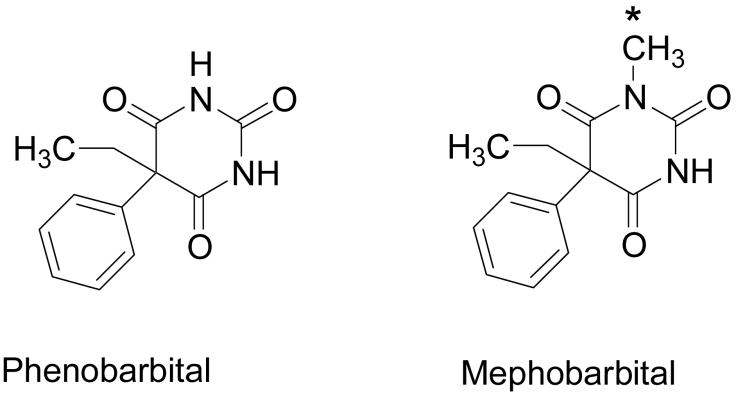

Figure 1.
Chemical structures of phenobarbital and mephobarbital. The ^{11}C-labelling position in mephobarbital is indicated by an asterisk.

Europe PMC Funders Author Manuscripts

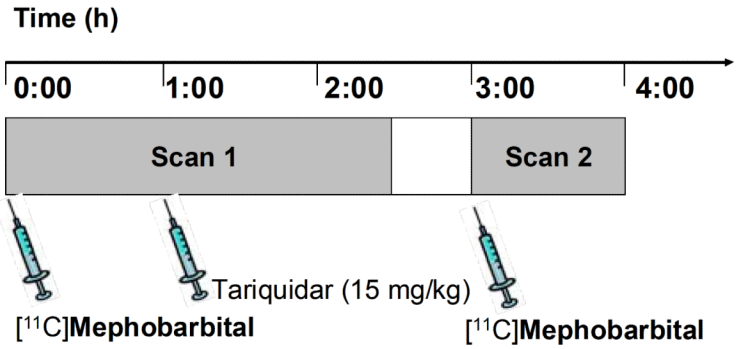

Figure 2.
Study set-up used in rats and mice. Scan 1 (150 min), during which the Pgp inhibitor tariquidar (15 mg/kg) was injected at 60 min after injection of [^{11}C]mephobarbital, was followed by scan 2 (60 min), which was recorded at 120 min after tariquidar administration.

Europe PMC Funders Author Manuscripts

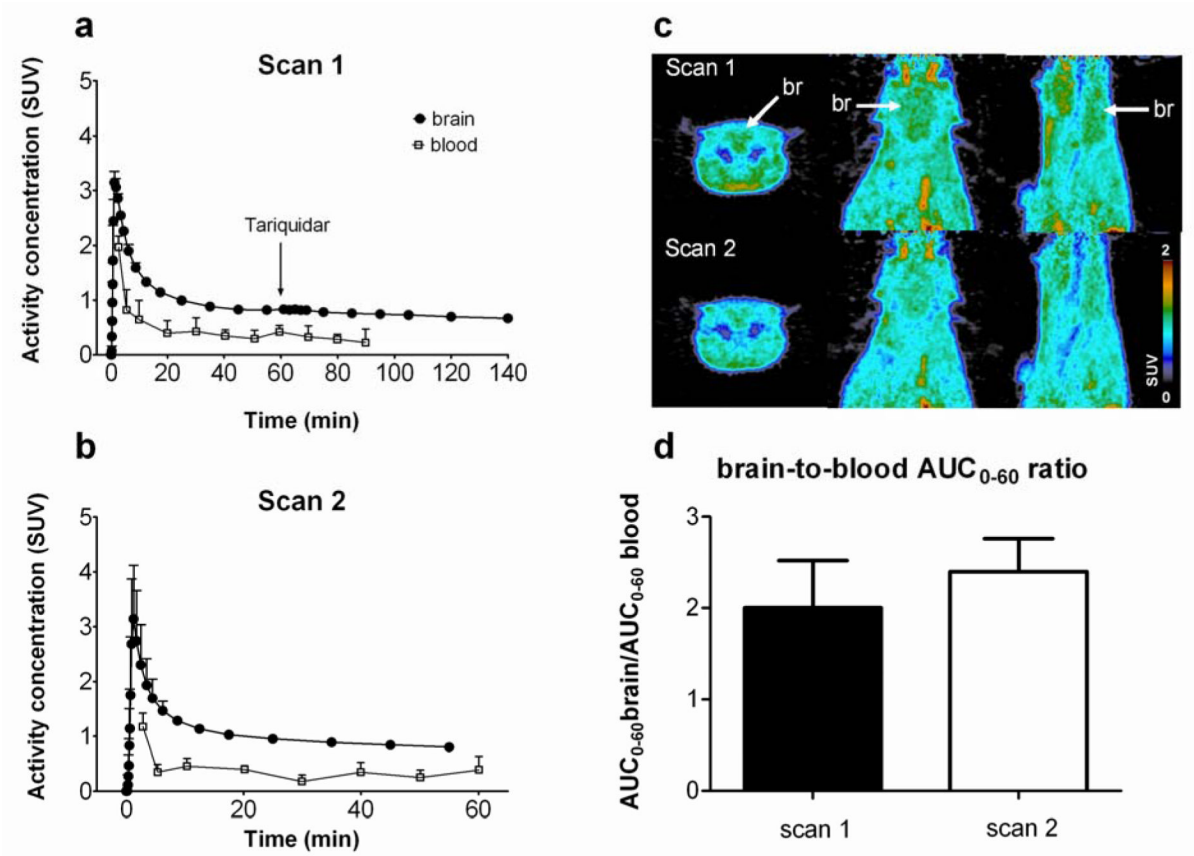

Figure 3.

In vivo evaluation of [^{11}C]mephobarbital in rats. (a) Mean (± SD, $n = 3$) time-activity curves in whole brain (filled circles) and arterial blood (open squares) for scan 1 and (b) scan 2. Activity concentration is expressed as standardized uptake value (SUV). The time point of tariquidar administration during scan 1 is indicated by an arrow. The arterial blood curves are only shown for time >3 min. (c) Representative PET summation images (0-60 min) for scan 1 and scan 2 in coronal, horizontal and sagittal planes (from left to right). Radiation scale is set from 0-2 SUV. The localization of the brain (br) is indicated by white arrows. (d) Mean (± SD, $n = 3$) brain-to-blood $AUC_{0\text{-}60}$ ratios for scan 1 and scan 2.

Europe PMC Funders Author Manuscripts

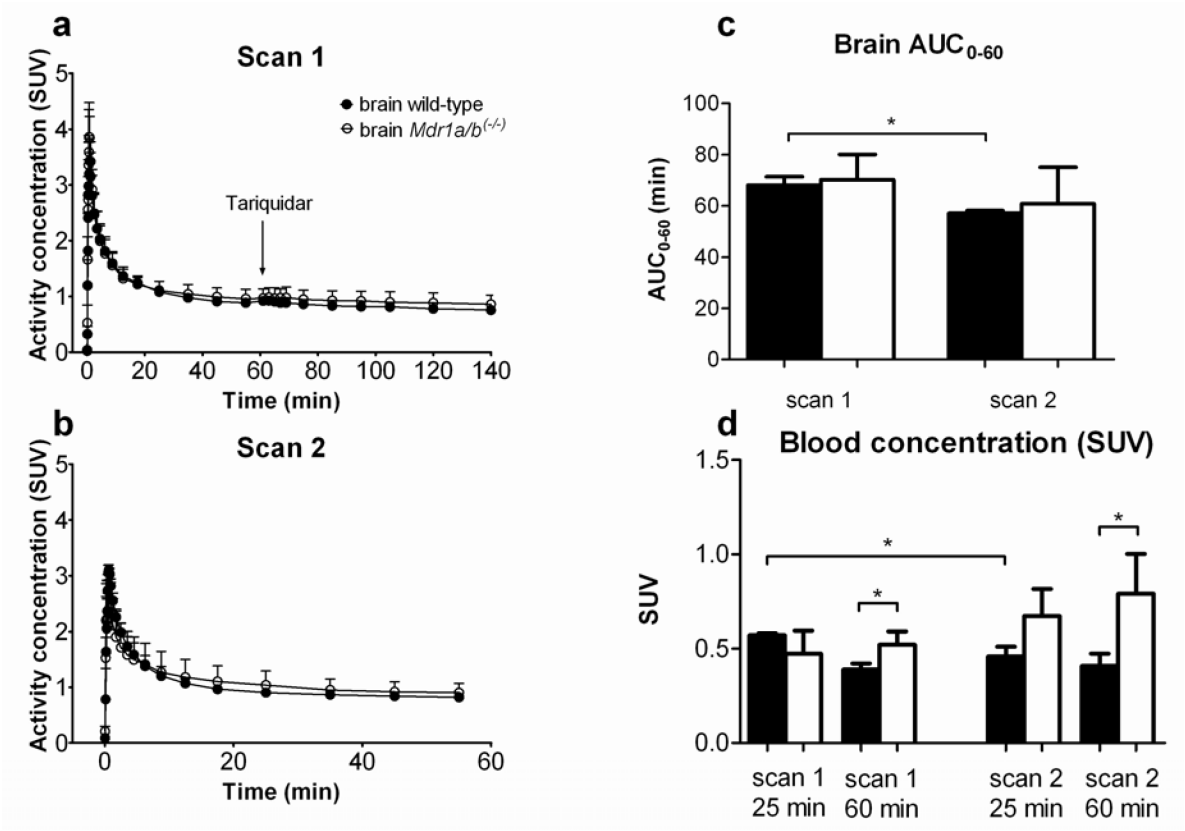

Figure 4.

In vivo evaluation of [^{11}C]mephobarbital in wild-type and *Mdr1a/b*$^{(-/-)}$ mice. (a) Mean (± SD, $n = 3$) time-activity curves in whole brain of wild-type mice (filled circles) and *Mdr1a/b*$^{(-/-)}$ mice (open circles) for scan 1 and (b) scan 2. Activity concentration is expressed as standardized uptake value (SUV). The time point of tariquidar administration during scan 1 is indicated by an arrow. (c) Mean (± SD, $n = 3$) $AUC_{0\text{-}60}$ values in whole brain of wild-type mice (black columns) and *Mdr1a/b*$^{(-/-)}$ mice (white columns). (d) Mean (± SD, $n = 3$) blood activity concentrations (SUV) at two time points (25 and 60 min) of scan 1 and scan 2 in wild-type mice (black columns) and *Mdr1a/b*$^{(-/-)}$ mice (white columns) measured in a separate group of animals than those used for the PET scans, * $p < 0.05$ (Student's t-test).

Europe PMC Funders Author Manuscripts

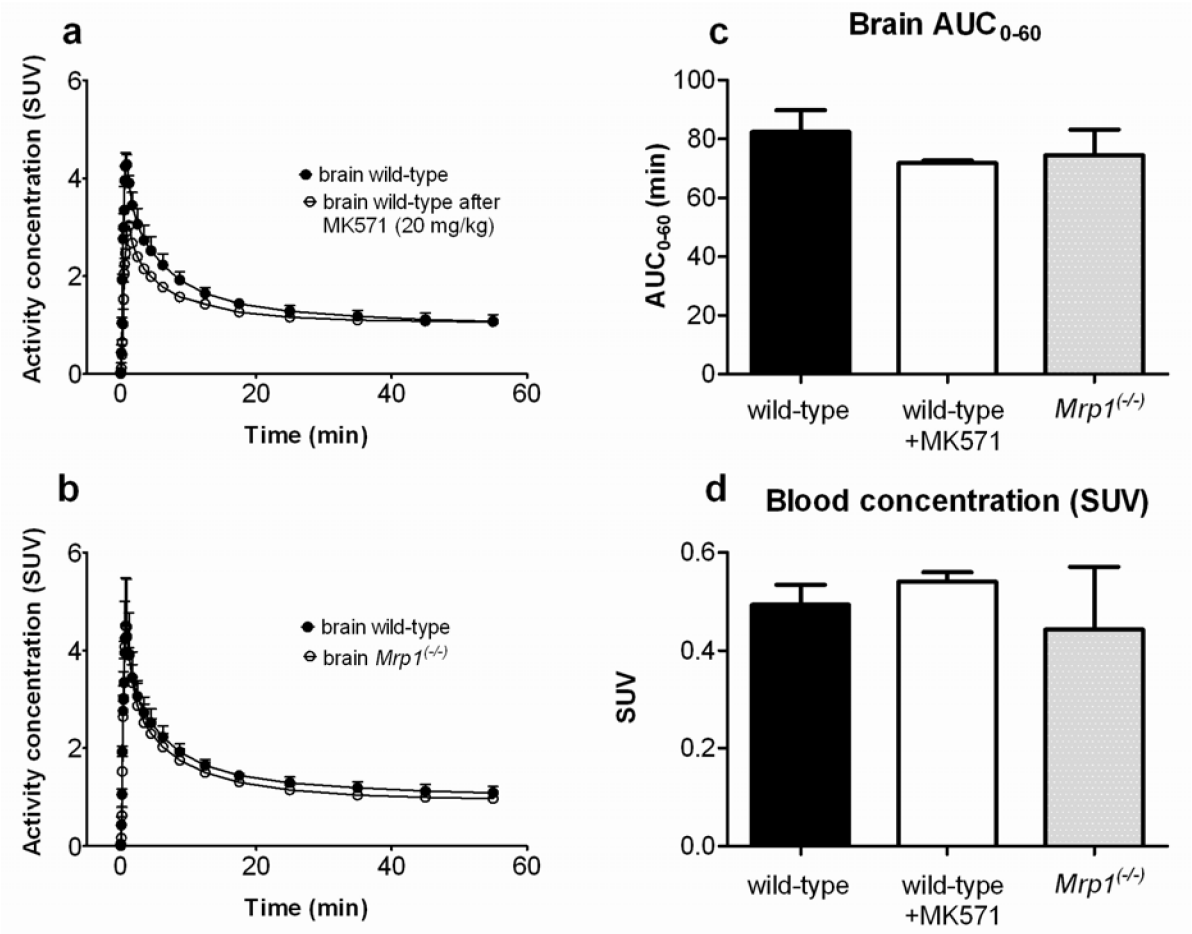

Figure 5.

In vivo evaluation of [^{11}C]mephobarbital in wild-type and *Mrp1*$^{(-/-)}$ mice. (a) Mean (± SD) time-activity curves in whole brain of wild-type mice without (filled circles, $n = 4$) and with (open circles, $n = 3$) pretreatment with the MRP inhibitor MK571 (20 mg/kg, iv). (b) Mean (± SD) time-activity curves in whole brain of wild-type mice (filled circles, $n = 4$) and *Mrp1*$^{(-/-)}$ mice (open circles, $n = 4$). Activity concentration is expressed as standardized uptake value (SUV). (c) Mean (± SD) $AUC_{0\text{-}60}$ values in whole brain of wild-type mice without (black column, $n = 4$) and with (white column, $n = 3$) pretreatment with MK571 (20 mg/kg, iv) and of *Mrp1*$^{(-/-)}$ mice (grey column, $n = 4$). (d) Mean (± SD) blood activity concentrations (SUV) in wild-type mice without (black column, $n = 4$) and with (white column, $n = 3$) pretreatment with MK571 (20 mg/kg, iv) and in *Mrp1*$^{(-/-)}$ mice (grey column, $n = 4$). Blood was collected at the end of the PET scan.

Europe PMC Funders Author Manuscripts

Europe PMC Funders Author Manuscripts

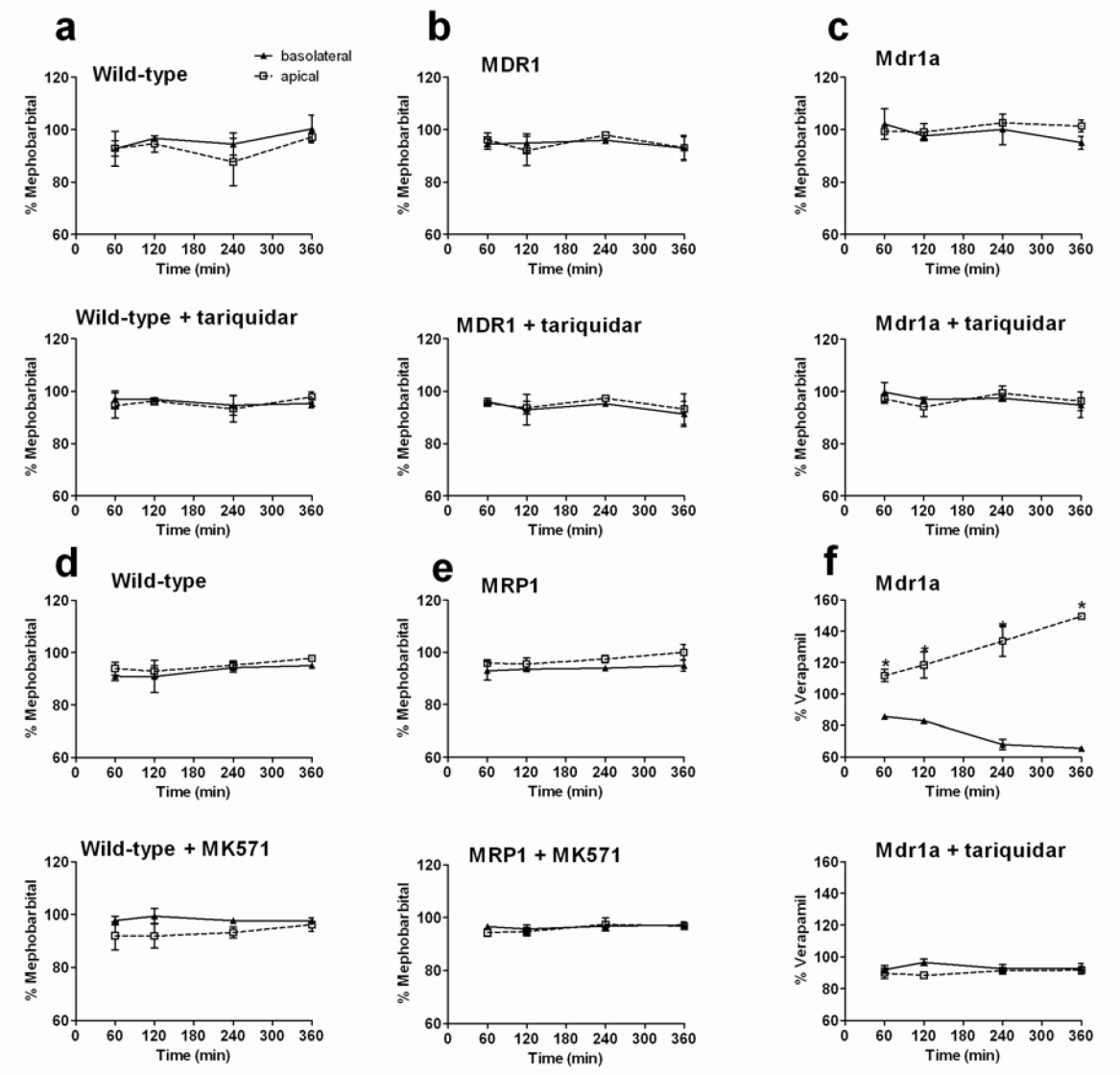

Figure 6.

Concentration equilibrium transport assay of mephobarbital (50 μM) in (a) wild-type LLC cells, (b) LLC cells transfected with human *MDR1* or (c) murine *Mdr1a* in presence (lower row) or absence (upper row) of the Pgp inhibitor tariquidar (0.5 μM). In (d) and (e) transport of mephobarbital in wild-type and human *MRP1*-transfected LLC cells in presence (lower row) and absence (upper row) of the MRP inhibitor MK571 (50 μM) is shown. The functional activity of Mdr1a was demonstrated by assessing transport of verapamil in presence or absence of tariquidar (f). Data are given as the mean (± SD, $n = 3$) percentage of the initial drug concentration (=100%) in either the apical or basolateral chamber *versus* time. Significant differences between the two chambers are indicated by asterisk (* $p < 0.05$).